mission lens. The magnitude of the bias error in this case is bounded, however, by the broadening error limit of Hanson. In this event, if the mean bias error is judged excessive, it could be removed by use of a calibration flow, to, in effect, determine the average fringe spacing at the receiving optics focus.

References

[1]Hanson, S., "Broadening of the Measured Frequency Spectrum in a Differential Laser Anemometer Due to Interference Plane Gradients," *Journal of Physics D: Applied Physics*, Vol. 6, No. 2, 1973, pp. 164–171.

[2]Hanson, S., "Visualization of Alignment Errors and Heterodyning Constraints in Laser Doppler Velocimeters," *Proceedings of the LDA Symposium* (Copenhagen), 1975, pp. 176–182.

[3]Durst, F., and Stevenson, W. H., "Moiré Patterns to Visually Model Laser-Doppler Signals," *Proceedings of the LDA Symposium* (Copenhagen), Hemisphere, Washington, DC, 1975, pp. 183–202.

[4]Durst, F., and Stevenson, W. H., "Properties of Focused Laser Beams and the Influence on Optical Anemometer Signals," *Proceedings of the Minnesota Symposium on Laser Anemometry*, Univ. of Minnesota, Dept. of Conferences, Minneapolis, MN, 1975, pp. 371–388.

[5]Young, W. H., Meyers, J. F., and Hepner, T. E., "Laser Velocimeter Systems Analysis Applied to a Flow Survey Above a Stalled Wing," NASA TN D8408, 1977.

[6]Rabe, D. C., and Dancey, C. L., "Comparison of Laser Transit and Laser Doppler Anemometer Measurements in Fundamental Flows," AIAA Paper 86-1650, June 1986.

New Supersonic Combustion Research Facility

M. R. Gruber* and A. S. Nejad†
U.S. Air Force Wright Laboratory,
Wright–Patterson Air Force Base, Ohio 45433

Introduction

A NEW research facility designed to allow studies of the basic mechanisms governing the mixing and combustion processes within realistic supersonic combustor geometries has been developed. With the push toward hypersonic flight regimes, such a facility provides a clear forum for enhancing the basic knowledge and databases through the use of conventional and advanced diagnostic techniques. The facility is capable of variable Mach number, continuous flow operation with a wide variety of conditions. Emphasis was placed on optical access to the nominally 5 × 6 in. test section; the resulting design utilizes four windows to allow visualization of all three orthogonal flow planes. Pitot rake studies reveal a uniform, two-dimensional, Mach 1.98 stream at the entrance to the test section. A slight decrease (2%) in freestream Mach number in the streamwise direction exists within the test section; however, the flow appears symmetric about the transverse and spanwise centerlines. Boundary-layer development is also documented.

Received Oct. 22, 1993; presented as Paper 94-0544 at the AIAA 32nd Aerospace Sciences Meeting and Exhibit, Reno, NV, Jan. 10–13, 1994; revision received Oct. 31, 1994; accepted for publication Dec. 5, 1994.

*Aerospace Engineer, Advanced Propulsion Division, Experimental Research Branch. Member AIAA.

†Senior Research Engineer, Advanced Propulsion Division, Experimental Research Branch. Member AIAA.

Facility Design

The underlying objective of this design effort was to develop an in-house research facility capable of allowing studies of the enhancement and control of fuel-air mixing in supersonic combustors with conventional and state-of-the-art, nonintrusive diagnostic techniques. Other design objectives of considerable importance were: variable Mach number, continuous flow operation, peak stagnation conditions of 400 psig and 1660°R at a peak flow rate of 34 lbm/s, nominal 5 × 6 in. test section with allowances for nozzle boundary-layer growth, high degree of optical access to the test section, modularity for ease of maintenance and future facility enhancement, and thermal expansion compensation to minimize test section movement. Figure 1a is a schematic of the result of the design effort, the design features are described in the following text.

Air Supply System

A series of compressors and a gas-fired heat exchanger are available to produce high-pressure/high-temperature air for use in the new laboratory. A hot line capable of supplying 17 lbm/s of 750-psig air at 1660°R and a cold line capable of supplying 17 lbm/s of 750-psig air at ambient temperature are used in tandem to produce the desired stagnation conditions. The two supply lines merge at a mixing station, and an insulated expansion loop transports the resulting mixed air to a supply manifold with five branches. Three branches supply air to the clean room, while the other two branches exit out through the roof (a vent line and a pressure relief line).

Flow Facility

Five major components comprise the combustion tunnel: 1) the inlet section, 2) settling chamber, 3) nozzle section, 4) test section, and 5) the diffuser (see Fig. 1a). All were designed in accordance with the ASME piping code.[1] The inlet section transports air from the supply manifold described above to the settling chamber. Six flexible stainless steel hoses connect the upper and lower manifolds and allow for thermal growth in the upstream direction. The lower manifold, block valve, and expansion section mount onto support carts that roll on a pair of rails. These carts allow for maintenance and additional thermal growth management. A rearward-facing perforated cone is housed within the expansion section to distribute the flow as it enters the 24-in. settling chamber.

The settling chamber uses an array of mesh screens and a section of honeycomb to condition the flow prior to acceleration by the supersonic nozzle. This chamber is designed to withstand 400 psig at 1660°R, while its size produces air velocities of approximately 50 ft/s over the range of desired tunnel operating conditions. Pressure and temperature sensors are installed to provide documentation and feedback to the control system. Finally, a transition region required by the change in geometry from the axisymmetric settling chamber to the planar nozzle section is housed at the downstream end of this chamber. The entire section mounts to a support stand that carries its weight and the force due to the subatmospheric pressure of the exhauster system.

Planar two-dimensional nozzles have been designed (M = 2, 3, 4.5) using a method of characteristics code developed by Carroll et al.[2] This code computes the contour of a continuous slope converging–diverging nozzle yielding a uniform exit flow aligned with the nozzle axis. Boundary-layer growth is not accounted for in this inviscid code. However, correction for viscous effects is accomplished using boundary-layer displacement thickness calculations resulting from Burke's equation,[3] which relates the local turbulent boundary-layer dis-

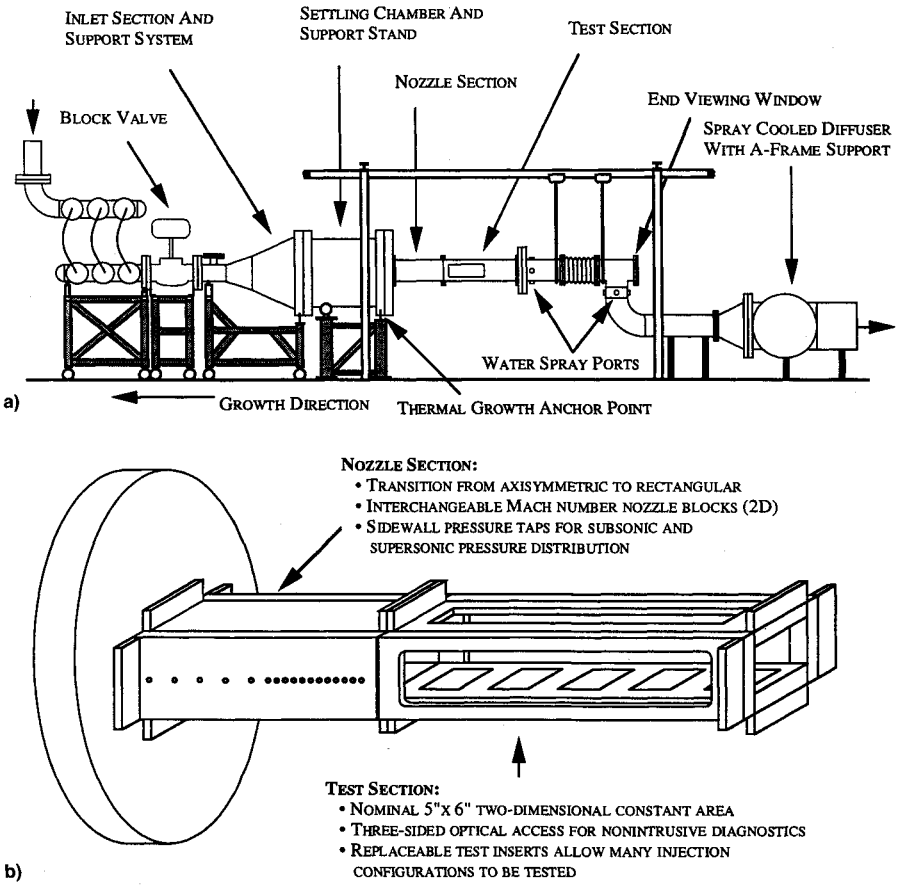

Fig. 1 Facility schematic: a) supersonic combustion tunnel and b) nozzle section/test section.

placement thickness to the local Mach and Reynolds numbers. This correction procedure assumes that the displacement thickness is zero at the nozzle throat and varies linearly with downstream position. Such a procedure introduces negligible errors into the correction.[4] After correction, the final nozzle exit dimensions are 5.16 × 6.00 in. A smooth contraction provides a transition from the exit of the nozzle flange to the throat.

The constant area test section requires a large degree of optical access so that a wide variety of nonintrusive diagnostic techniques may be used to probe the flow. A pair of side windows and a single top window provide the required access. Each window sits in its own frame and each frame has two orientations, one upstream and one downstream, to allow a total access of 31 in. along the streamwise dimension of the test section. The side windows offer access to the entire transverse dimension of the test section while the top window allows half of the spanwise dimension to be viewed directly. Appropriate safety considerations have been taken into account during the design of the windows,[5] which are made from fused silica. This material provides excellent transmissive properties in the uv wavelengths, which are commonly used in many of the diagnostic techniques slated for use in the facility. The bottom wall holds five removable test inserts positioned along the streamwise dimension of the test section. Various injection geometries and optical windows may be incorporated into these inserts so that a wide range of studies may easily be done. Figure 1b is a schematic of the test section showing the inserts and optical access.

The final component of the new facility is a spray-cooled diffuser section with a 9-in.-diam quartz access port positioned in the aft end allowing for visualization of the transverse–spanwise plane (end view) of the test section (see Fig. 1a). Water sprays cool the gases to levels below 660°R prior to reaching the facility coolers. Further details of the design process, along with a detailed overview of the control system hardware, may be found elsewhere.[6]

Calibration Techniques

Various conventional measurement techniques were used to characterize the facility. Pitot pressure rake studies examined the streamwise, transverse, and spanwise variations in the Mach number distribution within the test section. Wall static pressures were obtained from the nozzle section to examine the symmetry of the flow through the nozzle. Finally, boundary-layer rake profiles documented the boundary-layer growth on the test section bottom wall.

The pitot pressure rake used for the calibration studies could be incorporated into one of the removable test inserts of the bottom wall of the test section. This allowed the rake to be moved along the streamwise direction to any of the five available locations. The rake could also be traversed in the transverse direction. The probes were connected to a bank of Pressure Systems Incorporated pressure transducers. Signals from this system were collected by a personal computer and stored for future reduction. The nozzle sidewalls were equipped with pressure taps that allowed documentation of the centerline wall static pressure distribution from the contraction region entrance to the nozzle exit. The boundary-layer rake was mounted in place of the pitot rake on one of the test inserts and could be moved in the streamwise direction. Only the bottom wall profiles could be obtained (top wall window). The flow in the test section is relatively symmetric about the transverse centerline; thus, the bottom wall profiles are representative of the top wall also.

Calibration Results

Results of the pitot pressure rake studies are illustrated in Figs. 2a–2c. These figures show Mach number distributions

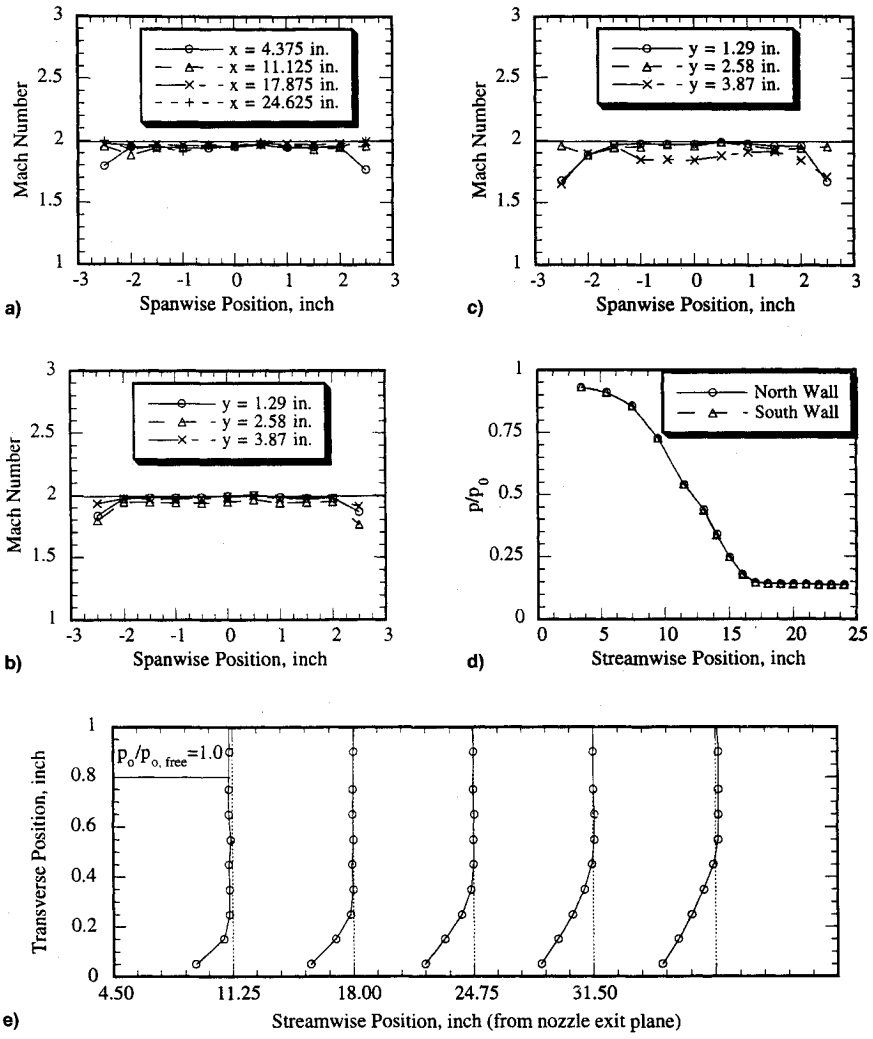

Fig. 2 Calibration results: a) streamwise and spanwise Mach number distributions at transverse centerline, b) transverse and spanwise Mach number distributions at x = 4.375 in., c) transverse and spanwise Mach number distributions at x = 11.125 in., d) pressure ratio profiles from nozzle sidewalls at P_0 = 52.8 psia, and e) contours of rake total pressure normalized by freestream total pressure.

across the span of the test section at various streamwise and transverse positions. Figure 2a shows Mach number distributions at the transverse centerline for four streamwise positions. The Mach number distribution is uniform for each position, but slightly decreasing with downstream distance from about 1.98 at the nozzle exit to about 1.95 at the final station. Figures 2b and 2c show the Mach number distributions across the span and height of the test section at two streamwise measurement stations. The position closest to the nozzle exit is documented in Fig. 2b. The Mach number distributions are very uniform across 4 in. of the span with a value of 1.98. This plot shows the symmetry of the flow about the transverse and spanwise centerlines as it exits the nozzle. Figure 2c presents the same three distributions at an intermediate streamwise location. Evidence of probe blockage is apparent at the highest transverse location; the two traces that do not exhibit this effect are again very symmetric about the spanwise centerline and uniform across about four inches of the test section.

Comparison of the two opposing nozzle sidewall pressure profiles gives some information concerning the symmetry of the flow about the spanwise centerline of the tunnel. Figure 2d illustrates the profiles obtained for a stagnation pressure of 52.8 psia. In the plot, the profiles of both north and south sidewalls are presented. As is clearly evident in the figure, both sidewall profiles fall on each other, suggesting spanwise symmetry through the nozzle.

The development of the bottom wall boundary layer is illustrated in Fig. 2e. The boundary-layer rake measured total pressures at enough transverse positions so that at least one measurement was made within the freestream, which yields the total pressure downstream of a normal shock at Mach 2. The plot in Fig. 2e shows transverse contours of measured total pressure normalized by the freestream measurement. The dashed lines show the individual streamwise measurement locations, and represent the locations where the pressure ratio takes a value of zero. At the first streamwise location, the boundary-layer thickness is about 0.2 in., while at the final measurement station, the boundary-layer thickness has grown to approximately 0.6 in.

Conclusions

A new research facility devoted to the study of the basic mechanisms governing mixing and combustion in realistic supersonic combustor geometries has been developed. This tunnel utilizes the large capacity air handling capabilities of the air facility to provide a continuous flow test environment within a nominally 5 × 6 in. test section. A high degree of optical access is available through the use of three windows around the test section and a fourth window at the downstream end of the diffuser. Such access allows visualization of all three orthogonal flow planes as well as numerous planes oblique to the mean flow. The usefulness of the new facility

has been demonstrated during recent injection studies.[7,8] Pitot rake measurements revealed a spanwise uniform and transversely symmetric Mach 1.98 flow exiting the nozzle section. Nozzle sidewall pressures suggested symmetry of the flow about the spanwise centerline of the tunnel. Finally, total pressure measurements just above the bottom wall illustrated boundary-layer growth.

References

[1]Anon., "ASME Boiler and Pressure Vessel Code B31.1, Section VIII, Unfired Pressure Vessels," American Society of Mechanical Engineers, 1989.

[2]Carroll, B. F., Dutton, J. C., and Addy, A. L., "NOZCS2: A Computer Program for the Design of Continuous Slope Supersonic Nozzles," Univ. of Illinois at Urbana–Champaign, UILU ENG 86-4007, Urbana, IL, 1986.

[3]Burke, A. F., "Turbulent Boundary Layers on Highly Cooled Surfaces at High Mach Numbers," Air Force Aeronautical Systems Div., AFASD TR 61-645, 1961.

[4]Fiore, A. W., Moore, D. G., Murray, D. H., and West, J. E., "Design and Calibration of the ARL Mach 3 High Reynolds Number Facility," Aeronautical Research Labs., TR 75-0012, 1975.

[5]Pope, A., and Goin, K. L., *High Speed Wind Tunnel Testing*, Wiley, New York, 1965.

[6]Gruber, M. R., and Nejad, A. S., "Supersonic Combustion Research Laboratory: Volume 1-Design and Fabrication," U.S. Air Force Wright Lab., WL-TR-93-2052, Wright–Patterson AFB, OH, 1993.

[7]Glawe, D. D., Donbar, J. M., Nejad, A. S., Sekar, B., Samimy, M., and Driscoll, J. F., "Parallel Fuel Injection from the Base of an Extended Strut into Supersonic Flow," AIAA Paper 94-0711, Jan. 1994.

[8]Gruber, M. R., Nejad, A. S., Chen, T. H., and Dutton, J. C., "Mixing and Penetration Studies of Sonic Jets in a Mach 2 Freestream," *Journal of Propulsion and Power*, Vol. 11, No. 2, 1995, pp. 315–323.

Planar Measurement of Absolute OH Concentration Distributions in a Supersonic Combustion Tunnel

T. M. Quagliaroli,* G. Laufer,† R. H. Krauss,‡ and J. C. McDaniel Jr.§
University of Virginia, Charlottesville, Virginia 22903

Introduction

NONINTRUSIVE diagnostic techniques have been shown to provide the necessary spatial resolution and the high measurement accuracy required for the validation of computational codes used to predict mixing and reaction in supersonic combustion facilities. Planar laser-induced fluorescence (PLIF) techniques are particularly suitable for the analysis of both nonreacting[1] and combusting gas flows[2] since they require only modest optical access and can provide the signal-to-noise ratio (SNR) and resolution required for accurate quantitative imaging. PLIF measurements involving molecular species naturally occurring in the flow, such as O_2, OH, and NO, have been used extensively for flow visualization and to determine two-dimensional velocity, temperature, and number density distributions.

OH PLIF has been used in a large variety of applications for measurements of velocity,[3] density, and temperature,[4] in both laminar and turbulent flames. Recently, a new approach for planar laser-induced fluorescence imaging of OH using a KrF excimer laser has been suggested[5] and demonstrated in a supersonic combustion facility.[6]

The objective of the present work was to demonstrate the KrF technique for quantitative PLIF imaging of OH concentration in a model H_2–air scramjet combustor. The fluorescence images were obtained following excitation by a KrF excimer laser operating at 248 nm, resonant with the $^2\Sigma^+(v' = 3) \leftarrow {}^2\Pi(v'' = 0)$ excitation band of OH. Absolute OH density distributions were obtained from the fluorescence images by using, as a reference source, the OH formed in a high-temperature electric furnace.[7] The effect on systematic error induced by collisional quenching by the major species has been assessed.

Theoretical Background

The fluorescence yield following the excitation of the $^2\Sigma^+(v' = 3) \leftarrow {}^2\Pi(v'' = 0)$ band in the A-X system of OH by a KrF laser has previously been evaluated theoretically for a range of temperatures and OH densities.[8] In a typical imaging PLIF experiment the total OH fluorescence in photoelectrons per pixel n_{pe} detected by an electronic camera consisting of an array having $n_p \times m_p$ pixels, increases linearly with its density, N_{OH}, and the relative occupational density of the probed state $\beta(T)$. However, the fluorescence signal is also a function of the spectroscopic properties of OH, as well as laser system and collection optics parameters. The uncertainty in determining these parameters limits the accuracy of the density measurement. Therefore, an independent PLIF measurement of N_{OH} in a calibrated OH source must be used to determine experimentally a calibration coefficient that is representative of system parameter effects and the spectroscopic coefficients.

The use of a high-temperature furnace to produce a stable, easily characterized source of OH for calibration of OH density measurements has recently been reported.[7] The OH fluorescence in this noncombusting environment has been shown[7] to result only from thermal dissociation of H_2O molecules. With known temperature, pressure, and relative humidity, equilibrium OH density in the furnace was calculated using the chemical equilibrium code STANJAN. Equilibrium OH mole fraction in excess of 10^{-4} was obtained. Having this density, direct relation between OH density and LIF quantum yield could be measured, using known laser pulse energy. The measured calibration coefficient accounts for the spectroscopic constants, optical, and geometrical parameters of the measurement, and laser beam parameters such as linewidth or locking efficiency. When the optical and geometrical parameters are identical for both the calibration and experimental measurements, N_{OH} can be determined by directly scaling the experimental photon count per unit laser energy by the predetermined calibration coefficient. A correction for the temperature dependence of $\beta(T)$ may be required, via the Boltzmann distribution. However, selection of an excitation transition with weak temperature dependence may allow for accurate density measurements without a prior temperature measurement.

Presented as Paper 93-0042 at the AIAA 31st Aerospace Sciences Meeting and Exhibit, Reno, NV, Jan. 10–14, 1993; received March 3, 1994; revision received Dec. 9, 1994; accepted for publication Dec. 17, 1994.

*Research Assistant, Aerospace Research Laboratory, Department of Mechanical and Aerospace Engineering, 570 Edgemont Rd. Student Member AIAA.

†Associate Professor, Aerospace Research Laboratory, Department of Mechanical and Aerospace Engineering, 570 Edgemont Rd. Senior Member AIAA.

‡Research Associate Professor, Aerospace Research Laboratory, Department of Mechanical and Aerospace Engineering, 570 Edgemont Rd. Member AIAA.

§Professor, Aerospace Research Laboratory, Department of Mechanical and Aerospace Engineering, 570 Edgemont Rd. Member AIAA.